

Performance of Standardized Precipitation Index (SPI) and Effective Drought Index (EDI) in Drought forecasting using Artificial Neural Networks (ANNs) for upper Tana River basin, Kenya

Raphael M. Wambua
Lecturer & PhD Candidate,
Department of Agricultural Egerton
University, Kenya,

Benedict M. Mutua
Associate professor, Department
of Agricultural Engineering,
Egerton University, Kenya

James M. Raude
BEED, Jomo Kenyatta
University of Agriculture and
Technology (JKUAT), Kenya

Abstract- Occurrence of drought events leads to water resources imbalance within a river basin. However, information on drought episodes for most basins such as Tana River basin in Kenya is limited. Due to the critical role of drought forecasting in early warning system and water resources planning and management, this paper presents the performance of Standardized Precipitation Index (SPI) and Effective Drought index (EDI) in drought forecasting using the Artificial Neural Networks (ANNs) for upper Tana River basin. The forecasting was conducted using various combinations of the past precipitation as input into the SPI and EDI functions in the proceeding forecasts. Numerous ANNs model architectures of SPI and EDI for 1, 3, 6, 9, 12, 18 and 24-months lead times were assessed for precipitation data from Mwea Irrigation and Agricultural Development (MIAD) Centre within the upper Tana River basin. The models were calibrated and validated using the correlation coefficient (R^2), Root-Mean Square Error (RMSE) and Mean Absolute Error (MAE). It was concluded that the optimum models forecast for EDI were found to be superior to SPI values with correlation coefficient (R^2) values ranging from 0.821 to 0.51 and 0.795 to 0.57 respectively for a 6- months lead time drought forecasting. The resulting forecasts of the Indices and ANNs models can be applied for timely drought early warning systems, water resources management and irrigation scheduling in upper Tana River basin.

Key words: Early warning system, SPI, EDI, Artificial neural networks, Lead time, Upper Tana River basin, Water resources management

I. INTRODUCTION

Drought is a condition on land characterized by recurring scarcity of water that falls below normal average or defined threshold levels [1]. Drought characteristics are critical in design, planning and management of water resources [2]. The term drought and its characteristics have been defined differently in numerous applications [3]. However, it is a challenge to quantitatively define the term. Droughts may be expressed in terms of indices using precipitation deficit, soil-water deficit, low stream flow, low reservoir levels and

low groundwater level. Different sectors use the terminology for different scenarios. For example, a hydrological-drought occurs whenever the river or groundwater levels are relatively low. In addition, water-resources drought occurs when basins experience low stream flow, reduced water reservoir volume and groundwater levels.

Droughts events cause direct or indirect negative impacts on river basins. This may include degradation of water resources in terms of quantity and quality, reduced agricultural production, increased soil erosion and land degradation, and increased plant diseases and insect attacks [1, 5]. Severe drought impacts experienced in numerous regions of the world lead to food insecurity and general increase in world food prices. Due to the mentioned problems of drought, river basin managers often have a critical role in addressing water risks, conflicts and enhancing economic development and simultaneously maintaining reliable water resources [6].

The water resources drought is influenced by climatic and hydrological parameters, characteristics of the water resource system and drought management practices. The hydrological drought, mainly deals with low stream flows. This drought adversely affects various aspects of human interest such as food security, water supply and hydropower generation [7, 8]. A sequence of droughts may lead to desertification of vulnerable areas such as arid, semi-arid and sub-humid areas. Within these fragile ecosystems, water resources, soil structure and soil fertility are critically degraded by drought occurrence [9]. The occurrence of any drought in terms of magnitude, duration and severity has not been clearly understood for numerous river basins in the world. To explicitly quantify, define and analyze drought, appropriate methods such as use of drought indices in conjunction with artificial neural networks can be applied.

II. CHARACTERISTICS OF DROUGHT

Droughts are characterized into numerous aspects. Some of the drought elements include drought severity, duration, frequency, magnitude and spatial distribution. Although these terms may be described differently, the following definitions provide their precise meaning. Drought severity refers to the extent of precipitation deficit in terms of magnitude or degree of impacts resulting from precipitation deficit [10]. In addition, Drought severity can be mathematically defined as a product of its magnitude and duration. Drought duration on the other hand refers to any continuous period of sequence with deficit of water below a defined truncation level. Intensity is the ratio of the

drought magnitude to its duration. Drought frequency also called return period of a drought is the mean time period between two consecutive drought events that have the same severity either equal or greater than a defined threshold. Magnitude refers to accumulated water deficit in terms of precipitation, soil moisture, runoff, stream flow, water reservoir levels and ground water below a certain truncation or threshold level for a given duration. Spatial distribution is the geographical extent in terms of areal coverage of drought which is variable during a drought event. These dimensions of drought are illustrated in Figure 1.

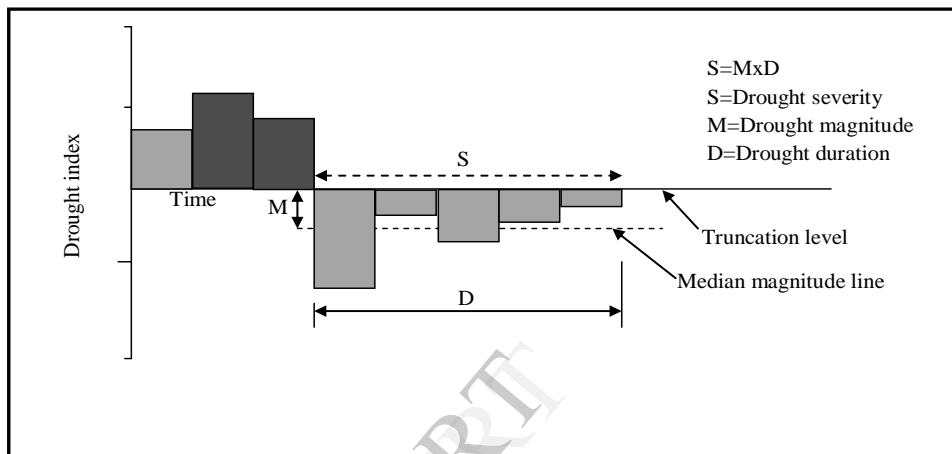


Fig. 1. Drought characteristics

III. DROUGHT INDICES

Drought indices or models are used for assessment of occurrence and severity of droughts. The Drought Indices (DIs) were developed for specific regions using specific structures and forms of data input. Drought indices may be categorized into two broad categories; remote-sensing based and the data driven drought indices [8]. The remote-sensing based indices are presented from data obtained from remote sensors to map the conditions of land. Data driven indices are those calculated using ground based data recorded over time [11, 12].

IV. ARTIFICIAL NEURAL NETWORKS IN DROUGHT FORECASTING

Artificial neural networks may be defined as a computational system with numerous processing elements whose operation is parallel [13]. These elements are interconnected based on specific architecture and have the capacity for self-modification of the connection weights each time the element parameters are being processed. The ANN model is similar to a biological neuron in that it has multiple input channels, data processing unit, and output channels called dendrites, cell body and the axon respectively as represented in Figure 2.

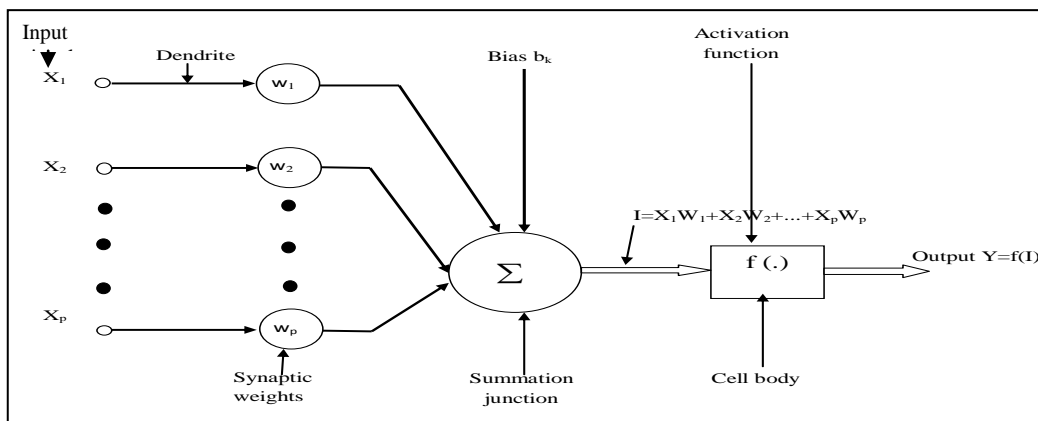


Fig. 2. Fundamental structure of typical neural network

The input signals given as (X_1, X_2, \dots, X_p) are passed to the neuron through the dendrites that represent different input channels. Each channel has its own weight referred to as connection weight denoted as W_1, W_2, \dots, W_p . The weights are very critical since they allow for collection and processing of signals based on their magnitude and effects on input functions. If a weight function gives a non-zero value at the synapse, it is allowed to pass through the cell body. Otherwise, if it has a value of zero, it is not allowed to pass the cell body. All the conveyed signals are normally integrated by summing up all the input [14]. Within the cell body, an activation function is used to analyze data input to yield output. ANN can be used to model linear and non-linear relationships [15]. Some of the networks such as recurrent networks process propagate and information in forward and backward directions through feedback loops [16, 17]. The study of drought forecasting, hydrology, water resource systems and numerous other aspects of Engineering and Science have received new outlook with invention, development and application of ANNs and drought indices [18]. The ANNs provide effective method of handling and processing of huge data sets in formulating relationships of complex natural and artificial systems.

The main objective of the research presented in this paper was to assess and compare the performance of SPI and EDI in drought forecasting at different lead times using Artificial Neural Networks based precipitation data for Mwea Irrigation and Agricultural Development (MIAD) station in the upper Tana River basin, Kenya.

V. MATERIALS AND METHODS

Description of the study area

The upper Tana River basin has an area of 17,420 km² and is part of the larger Tana River basin, which is the largest river system in Kenya with an area of 100,000 km² [19, 20]. Its forest land resources located along the eastern slopes of Mount Kenya and Aberdares range have a critical role in regulating the hydrology and hydro-power generation within the entire basin [21]. The upper Tana River basin lies between latitudes 00° 05' and 01° 30' south and longitudes 36° 20' and 37° 60' east (Figure 3). The basin is fundamental in influencing the ecosystem downstream. The focus of the present study is the Mwea Irrigation and Agricultural Development (MIAD) Centre which is located at latitude 0° 39.384' south and longitude 37° 17.402' east at an elevation of 1201 m above mean sea level as shown in Figure 3.

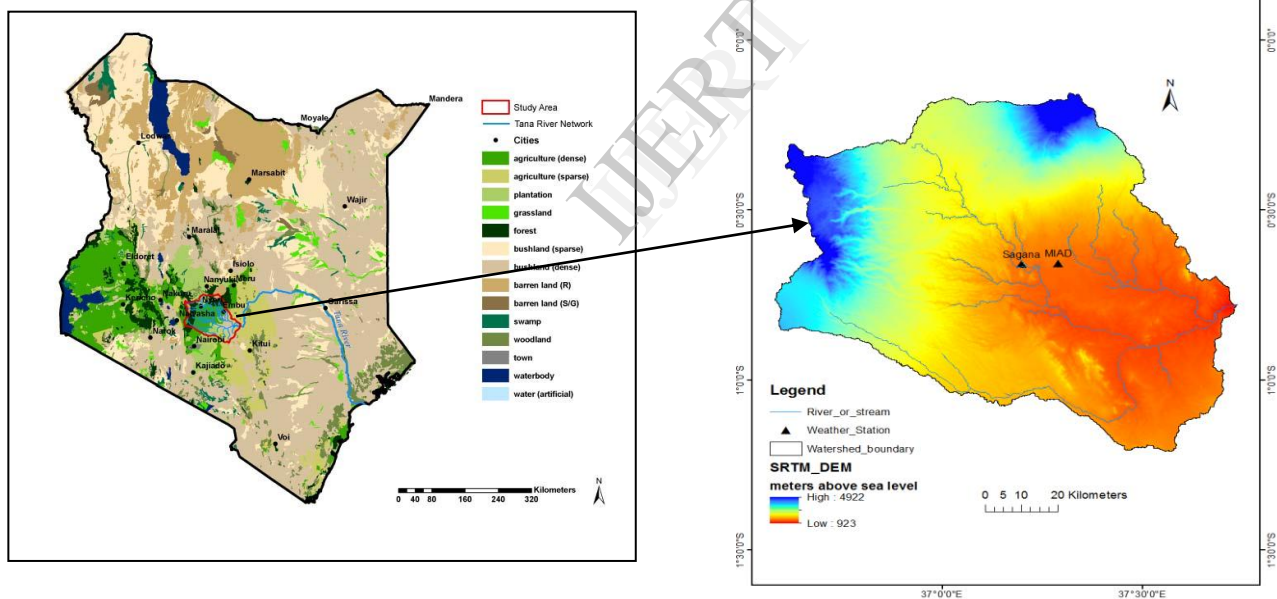


Fig. 3. The location of MIAD, Sagana stations and drainage network of the upper Tana River basin

VI. PRECIPITATION DATA AND SELECTED DROUGHT INDICES

To quantify drought using the SPI and EDI, monthly precipitation data from the MIAD station was used in this study. The MIAD station is located in Mwea irrigation scheme and it was perceived that drought monitoring would provide planning for water resources and irrigation scheduling. The data set for the MIAD station was for the period from August 2009 to June 2014. The Sagana meteorological station has data records for a longer period as compared to the MIAD station. The accuracy of the

rainfall data for both stations was first tested for homogeneity and trend using Mann-Kendall trend test technique [22, 23]. Since drought estimation requires data for a longer period, the MIAD data was correlated with the data for the same period as that of the Sagana meteorological station. The resulting regression equation yielded a correlation coefficient of 0.613 and is expressed as:

$$P_{MIAD} = 0.032 \times P_S^2 + 1.107 \times P_S + 0.481 \quad (1)$$

Where; P_{MIAD} is average amount of rainfall (mm) for i^{th} month at the MIAD station while P_S is the amount of

rainfall at the Sagana station. The function was used to estimate the rainfall for the period (1972-2014) and then used in computation of the drought indices. The SPI and EDI were computed for the MIAD station by applying the drought index package software as described by [23]. The package utilized numerous equations as described in the following sub-sections. The two indices used in the quantification of the drought are described below.

VII. COMPUTATION OF SPI

To calculate the SPI using the software package, the rainfall data was first fitted to the gamma distribution function. Then the data was transformed into a normal distribution to bring the mean SPI to zero [24]. The SPI values were computed for short-term (1 and 3 months), medium term (6 and 9 months) and long-term (12, 18 and 24 months) drought forecasting. For the SPI, the drought conditions are partitioned into near normal ($0.99 > \text{SPI} > -0.99$), moderate drought ($-1.0 > \text{SPI} > -1.49$), severe drought ($-1.5 > \text{SPI} > 1.99$) and extreme drought ($\text{SPI} < -2.0$). Drought was considered to begin when the SPI value reached -1.0 and the drought ends when it attained a positive value on a plot [24].

VIII. COMPUTATION OF EDI

The EDI was computed as a function rainfall required for a return to normal precipitation (RNP). The RNP was based on a principle of recovery of the rainfall from the accumulated deficit from the start of the drought event. Computation of EDI was done in a number of steps. The first step involved calculation of effective precipitation using the equation:

$$EP_p = \sum_{m=1}^N \left(\frac{\sum_{i=1}^m PE_m}{m} \right) \quad (2)$$

Where; EP_p is the effective precipitation parameter (mm), N is the duration of the preceding period (months), m is total period before the current month (months), PE_m is the effective precipitation in $m-1$ months before the current month (mm). The computation of EP when $N=1, 2, 3$ and 4 for instance were respectively formulated as:

$$EP_N = EP_{N-1} + \frac{(P_1 + P_2 + \dots + P_N)}{N} \quad (3)$$

$$EP_1 = \frac{P_1}{1} \quad (4)$$

$$EP_2 = EP_1 + \frac{(P_1 + P_2)}{2} \quad (5)$$

$$EP_3 = EP_2 + \frac{(P_1 + P_2 + P_3)}{3} \quad (6)$$

$$EP_4 = EP_3 + \frac{(P_1 + P_2 + P_3 + P_4)}{4} \quad (7)$$

Where EP_1, EP_2, EP_3 and $EP_4 EP_N$ are effective precipitation for $N=1, 2, 3, 4$ and n respectively while P_1, P_2, P_3 and P_4 are precipitation values during the current month, previous month, two and three months before respectively.

The mean and standard deviation of the resulting EP were then computed for every month. The time series of EP were then transformed to deviations from mean (DEP). Then the return to normal precipitation (PRN) values were calculated as a function of DEP using the relation:

$$PNR = \frac{DEP}{\sum \left(\frac{1}{N} \right)} \quad (8)$$

Where; N is the number of months. Suppose $N=2$ and $N=3$, then the summation reciprocal term is computed as:

$$\sum \left(\frac{1}{N} \right) = \frac{1}{1} + \frac{1}{2} = 1 \frac{1}{2}; \text{ For } N = 2 \quad (9)$$

$$\sum \left(\frac{1}{N} \right) = \frac{1}{1} + \frac{1}{2} + \frac{1}{3} = 1 \frac{5}{6}; \text{ For } N = 3 \quad (10)$$

The return to normal precipitation parameter was used to determine the EDI values using the following relation:

$$EDI = \frac{PRN}{Std(PRN)} \quad (11)$$

Where; $Std(PRN)$ is the standard deviation of each month's PRN. The resulting values were then used to categorize drought conditions. The EDI drought range adopted for this study include extreme drought ($\text{EDI} < -2.5$), severe drought ($-1.5 > \text{EDI} > 2.49$), moderate drought ($-0.7 > \text{EDI} > -1.49$) and near normal conditions ($-0.69 < \text{EDI} < 0.69$).

IX. ARTIFICIAL NEURAL NETWORKS (ANN)

The precipitation data was selected as the main input to the network for the two drought indices. The ANN was designed to model the relationship between the precipitation input and the outputs in form of drought indices. A Multi-Layer Perceptron (MLP) which is widely used for hydrological studies was adopted as the training algorithm. In the MLP structure, neurons were organized in interconnected layers. The three layers applied in the MLP structure are:

Input layer: this is a group of neurons where data input was introduced into the network.

Hidden layer: this is the set of neurons where the data is processed before being transmitted to the output layer.

Output layer: it consists of neuron where the results are displayed.

The above combinations of neurons were used to compute output response based on the weighted sum of all the inputs as per the activation function.

X. FORECASTING OF SPI AND EDI

All the input and output values were first standardized to range between 0.1 and 0.95 using the standardization equation:

$$X_n = X_{\min} + \frac{(X_o - x_{\min})}{(x_{\max} - x_{\min})} \times (X_{\max} - X_{\min})$$

(12)

Where; X_o is original variable value, X_n is the standardized value, x_{\min} is minimum value present in the original data set, x_{\max} is maximum value present in the original data set, X_{\min} is the selected minimum value for standardization (=0.1) and X_{\max} is the selected maximum value for standardization (=0.95).

Then SPI and EDI were forecasted by representing different combinations of their present and past values at different lead times calculated using past precipitation values. The forecasting was achieved within the ANN tool box of the MATLAB 2013a. The drought forecasting was achieved by constructing appropriate ANN models following numerous stages as shown in the following flow chart (Figure 4). To formulate the appropriate ANN architecture, the number of neurons and hidden layers were established. Various combinations of hidden layers and neurons were tested against R, RMSE and MAE criterion and the results summarized in Tables 1 and 2.

XI. RESULTS AND DISCUSSIONS

a) Time series drought conditions based on SPI and EDI.

The two indices exhibit the capacity to detect drought conditions ranging from extreme drought (SPI<-2.0, EDI<-2.5) to extremely wet conditions (SPI>2.0, EDI>2.5). From the time series plot of the observed and forecasted drought indices, the EDI generally respond gradually in detecting drought conditions compared to rapid response of SPI (Figures 5; c₁ and c₂). Considering the 6-months lead time, the EDI forecasts over-estimate the drought condition within the first 72 months. Within for the same period, the SPI forecasting accuracy is poor compared to the observed values. However the forecasting accuracy of both indices increases with time. The low accuracy at the beginning is attributed to the less data input into the models.

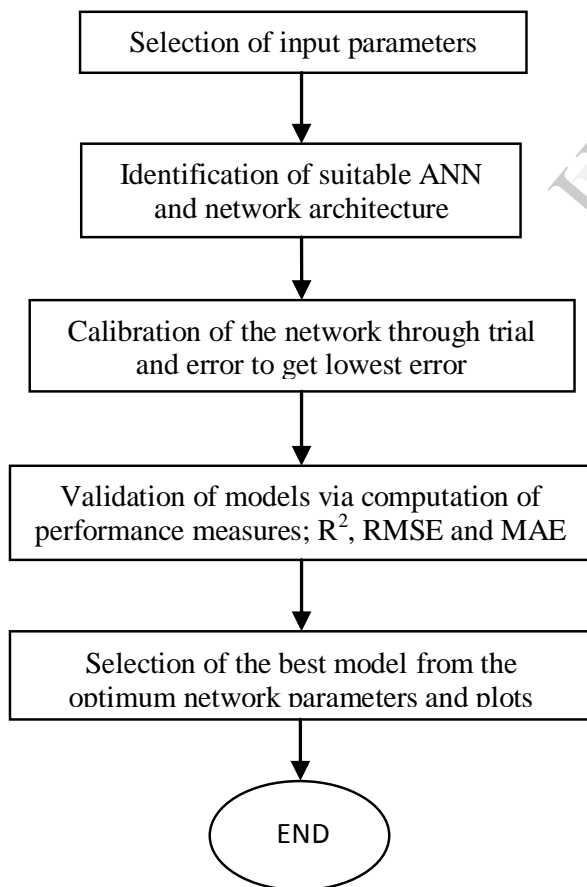
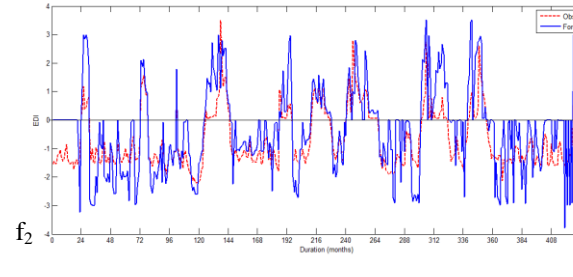
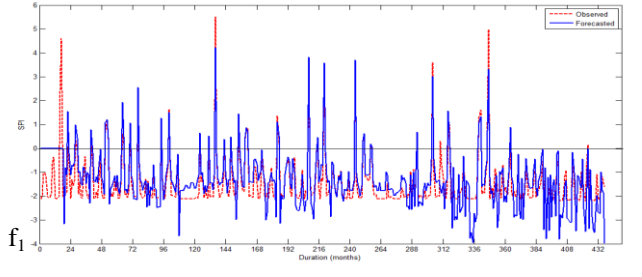
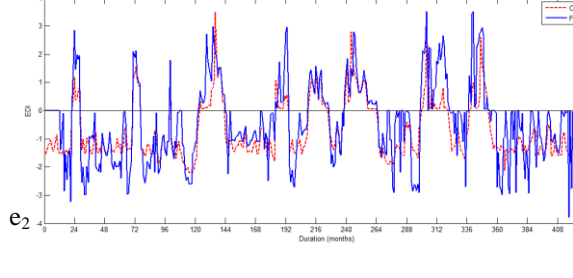
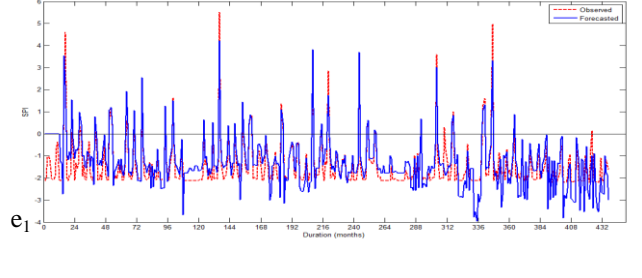
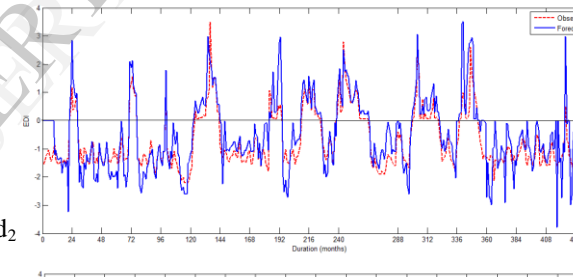
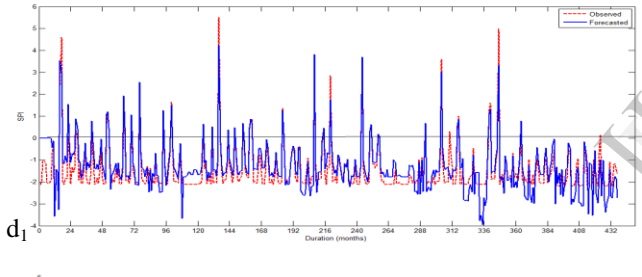
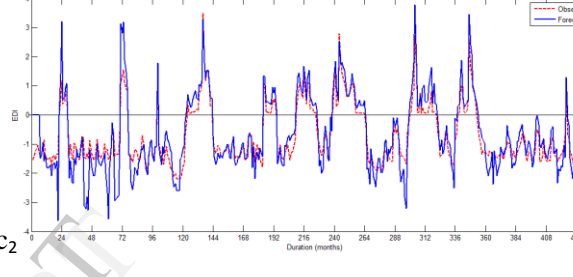
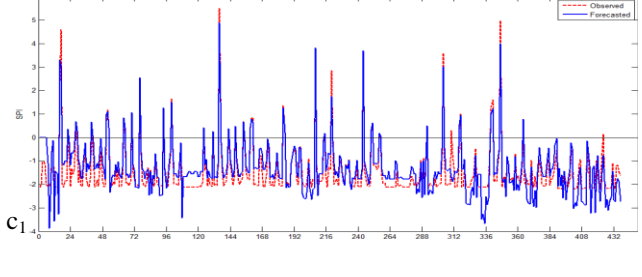
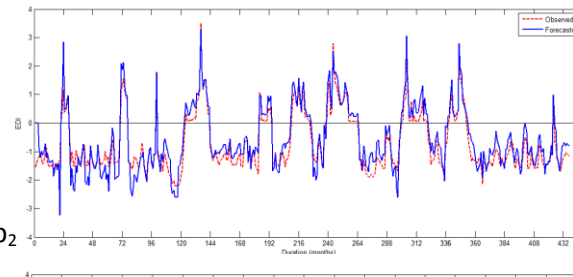
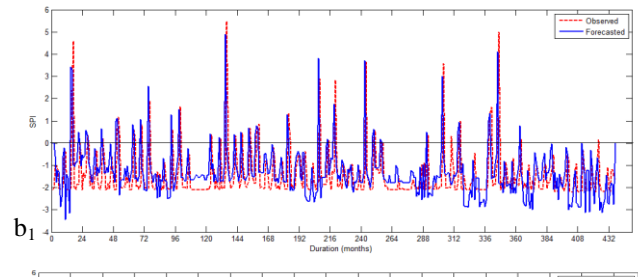
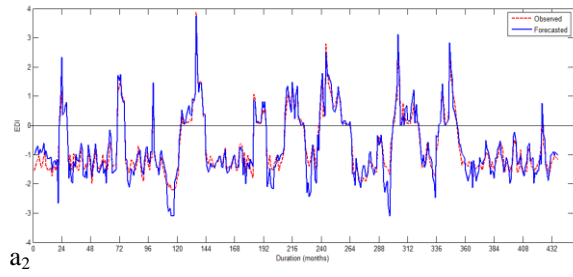
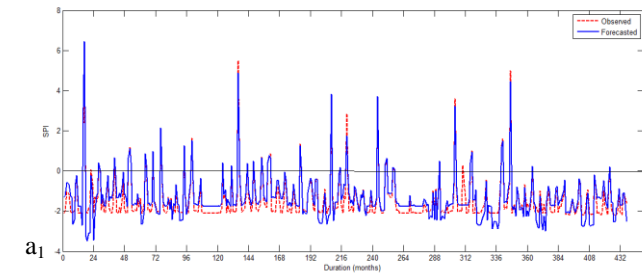


Fig. 4. Flow chart showing the summary of steps adopted for the ANN methodology



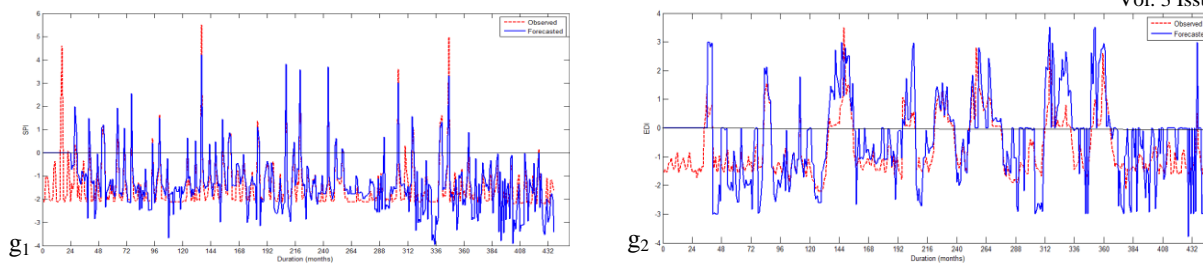


Figure 3.1 (a to g) : Comparison of observed and forecasted SPI and EDI at the MIAD station for 1,3,6,9, 12, 18 and 24-months lead time for the period 1972-2014

The statistics for model performance are summarized in the Table 2.1. The optimum model for 6-months lead time drought forecasting is trial 8 whose R^2 values for both calibration and validation are 0.79 and 0.70 respectively. Model 8 has also shown superior performance in forecasting drought for the 1, 3, 9, 12, 18 and 24-months lead times. The other lead model trials 4 and 2 performed better in forecasting drought with R^2 values of 0.57 and 0.48 respectively for SPI calibration.

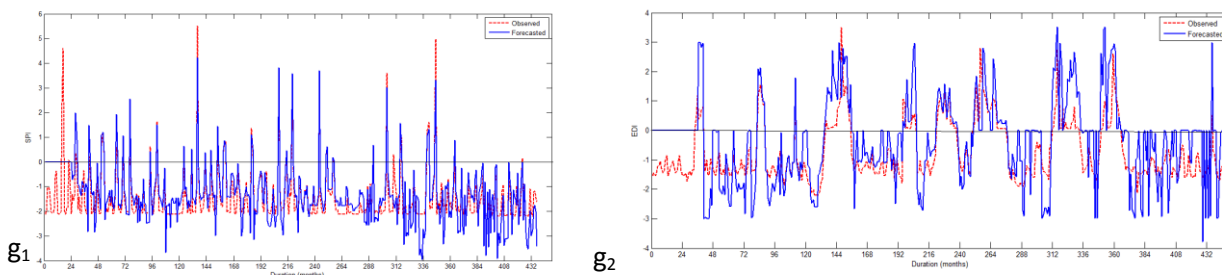


Fig. 5. Comparison of observed and forecasted SPI and EDI for 1, 3, 6, 9, 12, 18 and 24-months lead times at the MIAD station

Optimum drought forecasting was obtained for the EDI with model 6 whose architecture is the same as that of 8 in the SPI forecasting. Model 6 generated R^2 values of 0.82 and 0.75 for calibration and validation respectively. The results of the observed and the forecasted drought index values were plotted on regression graphs whose correlation equations are summarized in Table 3. Results indicate that the correlation coefficient decrease with forecasting lead time meaning that the models performance in forecasting

ability decline with lead time which is in agreement with results given by other researchers for other river basins [23]. Thus the highest models forecasting capability is for short-term, followed by medium-term and lastly long-term drought with R^2 values for SPI as 0.865, 0.795 and 0.472 respectively. Similar trend is presented for the EDI. However, the EDI performed better than the SPI forecasts with R^2 values ranging from 0.887 to 0.496 compared to 0.865 to 0.472 respectively (Table 3).

Table 1. Results of SPI forecasting for 6-months lead time at MIAD station

Input trial	ANN Architecture*	Calibration			Validation		
		R2	RMSE	MAE	R2	RMSE	MAE
1	6-2-1	0.35	0.84	0.66	0.16	1.32	0.89
2	6-3-1	0.48	0.48	0.74	0.38	0.78	0.65
3	5-2-1	0.45	0.91	0.73	0.19	1.36	0.73
5	6-2-1	0.39	0.88	0.92	0.17	1.02	0.76
4	5-3-1	0.57	0.43	0.61	0.47	0.66	0.45
6	6-4-1	0.47	0.93	0.75	0.34	0.77	0.61
7	4-3-1	0.32	0.89	0.56	0.15	1.06	0.87
8	5-6-1	0.79	0.37	0.19	0.70	0.49	0.32
9	5-4-1	0.31	0.88	0.54	0.35	0.69	0.59
10	6-3-1	0.44	0.90	0.74	0.28	1.58	1.13

*The three digits for architecture refer to number of neurons in input, hidden and output layers respectively. For instance the architecture 6-2-1 means six neurons in the input layer, two neurons in the hidden layer and one neuron in the output layer.

The SPI regression equations for the 1,3,9,12,18 and 24-months lead time are $y = 0.7594x + 0.14$, $y = 0.797x + 0.0112$, $y = 0.9053x + 0.2183$, $y = 0.8801x + 0.2321$, $y = 0.9025x + 0.2319$ and $y = 0.899x + 0.2246$. On the other hand EDI Regression equations for the lead times are $y = 0.9411x + 0.1185$, $y = 0.9501x + 0.1141$, $y = 0.9202x + 0.2231$, $y = 0.9616x + 0.222$, $y = 0.9793x + 0.2244$ and $y = 0.9574x + 0.2253$ respectively.

The correlation coefficient for both indices declined with lead time (Table 3). The R² values of the observed and

forecasted SPI and EDI are 0.795 and 0.821 respectively for the 6-months lead time (Figure 5).

b) Comparison of SPI and EDI forecasts

The results show that the validation statistics used for 1, 3, 6, 9, 12, 18 and 24-months lead time such as R², RMSE and MAE are superior for the EDI compared to the SPI (Figure 6). This is linked to the difference in response of the SPI and EDI to rainfall as illustrated in (Figure 6). The SPI peaks have immediate fluctuations while the EDI peaks are slow. The dawdling response may be attributed to the EP parameter which is an indicator of antecedent precipitation event for smooth response of the EDI to time series precipitation fluctuations.

Table 2. Results of EDI forecasting for 6-months lead time at MIAD station

Input trial	ANN Architecture	Calibration			Validation		
		R2	RMSE	MAE	R2	RMSE	MAE
1	5-3-1	0.51	0.39	0.56	0.48	0.59	0.44
2	6-3-1	0.43	0.74	0.58	0.34	0.76	0.65
3	5-2-1	0.35	0.85	0.68	0.19	1.37	0.74
4	4-3-1	0.59	0.52	0.25	0.46	0.64	0.57
5	6-2-1	0.47	0.48	0.37	0.34	0.71	0.61
6	5-6-1	0.82	0.32	0.211	0.75	0.53	0.36
7	4-3-1	0.38	0.83	0.88	0.44	0.68	0.34
8	5-4-1	0.41	0.77	0.89	0.36	0.79	0.64
9	6-4-1	0.48	0.49	0.35	0.26	1.48	1.12
10	6-2-1	0.32	0.86	0.52	0.37	0.74	0.65

*The three digits for architecture refer to number of neurons in input, hidden and output layers respectively. For instance the architecture 5-3-1 means five neurons in the input layer, three neurons in the hidden layer and one neuron in the output layer.

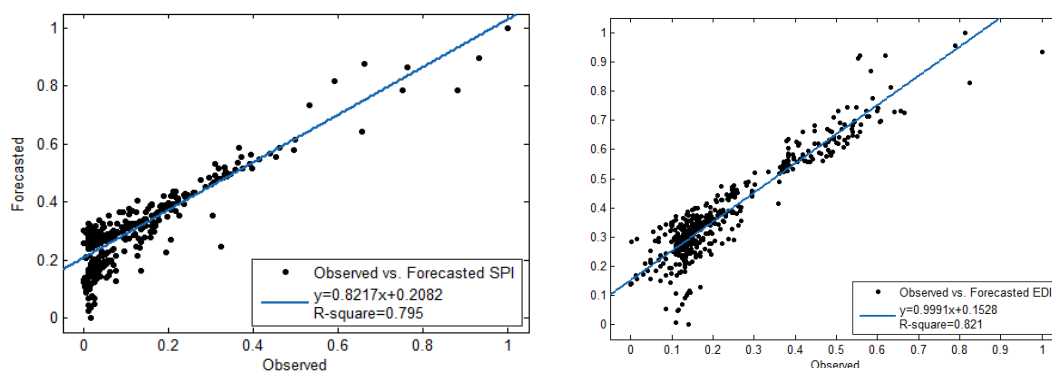


Fig. 5. Regression between the observed and the forecasted 6-months SPI and EDI for MIAD Station based on the ANN toolbox

Table 3. Summary of correlation coefficients of SPI and EDI for different lead times

Lead time (months)	Correlation coefficient (R^2)		Drought forecasting period
	SPI	EDI	
1	0.865	0.887	Short-term
3	0.816	0.854	Short-term
6	0.795	0.821	Medium-term
9	0.671	0.744	Medium-term
12	0.587	0.627	Long-term
18	0.519	0.594	Long-term
24	0.472	0.496	Long-term

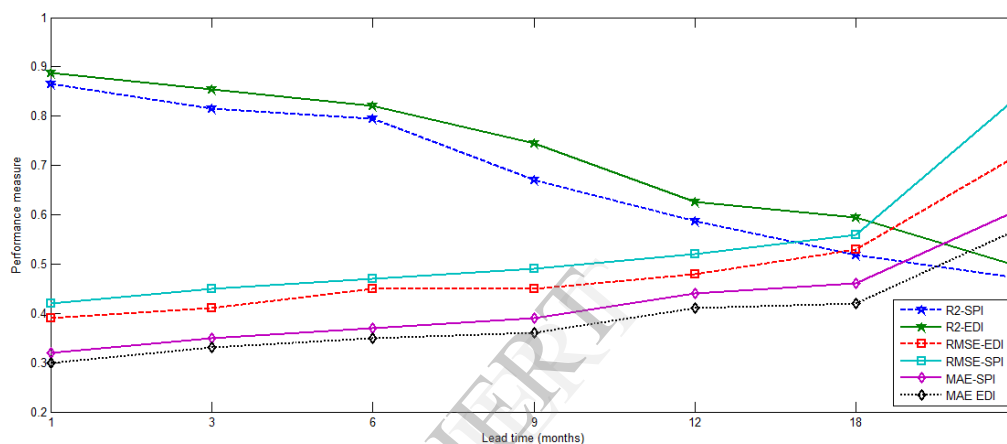


Fig. 6. Comparison of the SPI and EDI forecast at different lead times

XII. CONCLUSION

Results show that as the forecast lead time is increased, the correlation between observed and predicted values decrease as determined by decrease in the R^2 and increase in RMSE values. In addition, there is a reduced sensitivity to changes in monthly precipitation for the EDI time series forecasts compared to those of the SPI. Reduction in sensitivity is more prominent in long-term EDI as they are less sensitive to monthly precipitation than the short-term EDI.

Different network models were tested for the SPI and EDI at the MIAD rainfall station in the upper Tana River basin. The optimum ANN models for both the SPI and EDI exhibit simple network architecture. Generally three layer networks were explored for their forecasting capability. The network with six neurons of the hidden layer was found to be optimum for MIAD station and the 1, 3, 6, 9, 12, 18 and 24 months lead times. The best models developed in the present findings gave R^2 values of 0.79 and 0.82 for SPI and EDI respectively. This indicates that EDI has a higher drought forecasting accuracy than the SPI.

Based on the statistical principles used in study (R^2 , RMSE and MAE), the EDI is more effective in drought forecasting than the SPI for different lead times. In addition, the EDI presented a gradual response to drought on-set, development and cessation, while at the same time accurately forecasting patterns of drought classes. It is paramount to apply the findings of the drought forecasting and build it into drought early warning systems and water resources planning and management at the Mwea Irrigation and Agricultural Development (MIAD) centre.

XIII. ACKNOWLEDGEMENT

The authors acknowledge the partial financial support by the Division of Research and Extension, Egerton University. The financial support provided by the University in publishing the findings as per this article from a wider research project is greatly appreciated.

REFERENCES

- [1] Wambua, R. M., Mutua, B. M. and Raude, J. M. (2014). Drought forecasting using indices and artificial neural networks for upper tana river basin, Kenya -A review concept, *Journal of Civil and Environmental Engineering*, 4(4): 1-12.
- [2] Kyambia, M. and Mutua, B. M. (2014). Analysis of drought effect on annual stream flow of river Malewa in lake Naivasha basin, Kenya, *International Journal of Current Research and Reviews*, 6(18): 1-6.
- [3] UNDP. (2012). Kenya : adapting to climate variability in Arid and Semi-Arid Lands (KACCAL), project report Wilby, R. L., Orr, H. G., Hedger, M, Forrow D. and Blakmore, M. (2006a). Risks posed by climate variability to delivery of water framework directive objectives. *Environ. Int.*, in press.
- [4] UN. (2008). Trends in sustainable development, agriculture, rural development, land desertification and drought. Department of economic and social affairs, United Nations, New York.
- [5] Scheffran, J., Marmer, E., and Show, P. (2012). Migration as a contribution to resilience and innovation in climate adaptation: social networks and co-development in North West Africa, *applied geography*, 33: 119-127.
- [6] Okoro, B. C., Uzoukwu, R. A. and Chiomezie, N. M. (2014). River basins of Imo State for sustainable water resources management, *Journal of Civil and Environmental Engineering*, 4(1): 1-8.
- [7] Karamouz, M., Pasaouli, K. and Wzif, S. (2009). Development of a hybrid drought prediction, a case study, *J. Hydro Eng.* 14(6): 617-627.
- [8] Belayneh, A. and Adamowski, J. (2013). Drought forecasting using new machine learning methods, *Journal of Water and Land Development*, 18 (I-IV): 3-12.
- [9] El-Jabi, N., Turkkan, N. and Caissie, D. (2013). Regional climate index for floods and droughts using Canadian climate model, *American journal of climate variability*, 2: 106-115.
- [10] Wilhite, D. A. (2004). Drought as a natural hazard, in international perspectives on natural disasters ; occurrence, mitigation, and consequences, edited by J. P. Stollman, J. Lidson and L. M. Dechano, Kluwer academic publishers, the Netherlands: 147-162.
- [11] Mulla, D. (2013). Twenty five years of remote sensing in precision agriculture: key advances and remaining knowledge gaps, *Journal of Biosystems Engineering*, 114 (4): 358-371.
- [12] Sayanjali, M. and Nabdell, O. (2013). Remote sensing satellite design using model based system Engineering, *Journal of Science and Engineering*, 1(1): 43-54.
- [13] Dhande, E. S. and Mane, S. J. (2014). Wastewater quality forecasting by using artificial neural network, *International Journal of Engineering Research and Technology (IJERT)*, 3(9): 1508-1511.
- [14] Barua, S. (2010). Drought assessment and forecasting using a non-linear aggregated drought index, PhD thesis, Victoria University, Australia.
- [15] Chai, S. S. (2010). An Artificial Neural Network approach for soil moisture retrieval using passive microwave data, PhD thesis, Curtin University of Technology.
- [16] Timm L. C., Gomes D. T., Barbosa E. D., Reichardt K., Souza M. D. and Dynia J. F. (2006). Neural Network and state space models for studying relationship among soil properties, *J. Scientia Agricola*, 63: 386-395.
- [17] Chiang, Y.M, Chang, L. C. and Chang, F. J (2004). Comparison of static feed forward and dynamic feedback neural networks for rainfall runoff modelling, *Journal of Hydrology*, 290(3-4): 297-311.
- [18] Cutore, P., Mauro, G. D. and Cancelliere, A. (2009). Forecasting Palmer index using artificial neural networks and climate indices, *journal of Hydrologic Engineering*, 14(6): 588-595.
- [19] Jacobs, J. Angerer, J., Vitale, J., Srinivasan, R., Kaitho, J. and Stuth, J. (2004). Exploring the Potential Impact of Restoration on Hydrology of the Upper Tana River Catchment and Masinga Dam, Kenya, a Draft Report, Texas A & M University.
- [20] WRMA. (2010). Physiological survey in the upper Tana river catchment, a natural resources project report, Nairobi.
- [21] IFAD, (2012).Upper Tana Catchment natural resources management projects report east and southern Africa division, project management department.
- [22] Xiong, L. and Guo, S. (2004). Trend test and change-point detection for the annual discharge series of the Yangtze river at the Yichang hyd. Station *Hydrological Sci.* 49(1): 99-112.
- [23] Morid, S. Smakhtin, V. and Bagherzadeh, K. (2007). Drought forecasting using artificial neural networks and networks and time series of drought indices *International Journal of climatology*, 27 (15): 2103-2111.
- [24] Mckee, T. B., Doesken, N. J. and Kleist, J. (1993). The relationship of drought frequency and duration to time scales in proceedings of 8th conference on applied climatology, Anaheim, California, U.S.A.,179-184.